



Sesquiterpene lactones; Damsin and neoambrosin suppress cytokine-mediated inflammation in complete Freund's adjuvant rat model via shutting Akt/ERK1/2/STAT3 signaling

Shymaa I.A. Abdel-dayem^{a,*}, Mohammed N.A. Khalil^{a,b}, Enas H. Abdelrahman^a, Hamida M. El-Gohary^a, Ahmed S. Kamel^c

^a Pharmacognosy Department, Faculty of Pharmacy, Cairo University, Kasr El-Aini, Cairo, 11562, Egypt

^b Pharmacognosy Department, Faculty of Pharmacy, Heliopolis University, Cairo, 11361, Egypt

^c Pharmacology Department, Faculty of Pharmacy, Cairo University, Kasr El-Aini, Cairo, 11562, Egypt

ARTICLE INFO

Keywords:

Damsin
Neoambrosin
Rheumatoid arthritis
Complete Freund's adjuvant
Akt/ERK1/2/STAT3 pathway

ABSTRACT

Ethnopharmacological relevance: Although Damsissa (*Ambrosia maritima*) is traditionally used as anti-inflammatory and diuretic, the biological activity and mechanism of action of its major constituents are to be elucidated.

Aim: to decipher the anti-arthritis potential of damsine (DMS) and neoambrosin (NMS) and to unfold their molecular signaling in complete Freund's adjuvant (CFA)-induced arthritis model.

Materials and methods: the right hind paw was inoculated with CFA (0.1 ml) at day 0 and 7 while treatments were started from the 14th day and continued for 2 weeks. Rats were randomly assigned into 4 groups; normal group (NRML), CFA-induced arthritis group, CFA-induced arthritis treated with DMS and NMS (10 mg/kg/day) as 3rd and 4th group; respectively.

Results: Throughout experimental period, treatments ameliorated the increase of paw volume, knee joint diameter and nociception tests as reflected in open field arena. Also, DSM and NMS suppressed phosphorylation of Akt, STAT-3, ERK1/2 which was further mirrored by inactivation of GSK3 β and downregulation of MCP-1 together with CCN1 and NF- κ B in hind paw tissue. Concomitantly, inflammation markers; TNF- α , IL-6, -12 were lowered as confirmed microscopically during examination of hind paw tissue.

Conclusion: DSM and NMS-induced suppression of NF- κ B subdues clinical features of RA most probably through repression of Akt/ERK1/2/STAT3 pathway. Therefore, DMS and NMS can serve as safe and effective treatment for rheumatoid arthritis, one of the most disabling chronic, inflammatory and painful autoimmune disease.

1. Introduction

Rheumatoid arthritis (RA) is a chronic autoimmune inflammatory joint disorder characterized by articular symptoms such as synovial inflammation, swelling, joint stiffness and immobility that ultimately ends with deleterious systemic effects on body weight, cardiovascular, pulmonary and skeletal systems. Epidemiologically, it has prevalence rate of 5 per 1000 individual with the females are more prone to the disease and can occur at any age although its maximal incidence occurs in sixties (Aletaha and Smolen, 2018). The disorder has socioeconomic burden because of the functional disabling disorder that appears in the early phase of the disease with significant impact on the daily life

aspects. This dramatically affects the quality of life of the afflicted patients.

It is observed that significant proportion of patients are not managed nor controlled effectively by the current therapies (Guo et al., 2018; Rubbert-Roth and Finckh, 2009). This lack of patients' response may be owed to the unknown etiology of the disease and presence of different contributing factors viz, environmental and genetic ones (Calabresi et al., 2018). However up to date, no consistent hypothesis contains all these elements can depict the pathophysiology of the disease. On the other hand, the high cost and long-term associated adverse effects represent a challenge and limitation in the choice of treatment strategies. In response to the harmful consequences of RA and/or drug-induced harmful effects, the attention of the researchers jumps to

* Corresponding author. Pharmacognosy department, Faculty of Pharmacy, Cairo University, Kasr el Aini St., P.B, 11562, Cairo, Egypt.

E-mail addresses: shymaa.aly@pharma.cu.edu.eg, shymaaabdeldayem@gmail.com (S.I.A. Abdel-dayem), mohamed.nabil@pharma.cu.edu.eg (M.N.A. Khalil), enas.abdelrahman@pharma.cu.edu.eg (E.H. Abdelrahman), h.elgohary@hotmail.com (H.M. El-Gohary), ahmed.seifeldin@pharma.cu.edu.eg (A.S. Kamel).

<https://doi.org/10.1016/j.jep.2020.113407>

Received 2 February 2020; Received in revised form 15 September 2020; Accepted 17 September 2020

Available online 23 September 2020

0378-8741/© 2020 Elsevier B.V. All rights reserved.

Abbreviations

CFA	Complete Freund's Adjuvant
RA	rheumatoid arthritis
NRML	normal groups
DCM	dichloromethane
ETOAc	ethyl acetate
ACN	acetonitrile
DMS	damsin
NMS	Neoambrosin
Akt	protein kinase B
PI3K	Phosphoinositide 3-kinases
ERK1/2	Extracellular signal-regulated kinases

GSK3 β	Glycogen synthase kinase 3 beta
STAT3	Signal transducer and activator of transcription 3
MCP-1	Monocyte chemoattractant protein-1
CCL2	chemokine (C-C motif) ligand 2
CCN1	Cellular Communication Network Factor 1
Cyr61	cysteine-rich 61
FOXO3a	Forkhead box O3
Tyr705	Phospho-Stat3 (Tyr705) Antibody
IL-6	interleukin-6
NF-k β	nuclear factor kappa-light-chain-enhancer of activated β cells
TNF- α	tumor necrosis factor alpha
ANOVA	Analysis of variance

spot safe, effective and tolerable compounds to alleviate RA.

Ambrosia maritima, commonly known as damsisa, is traditionally used as diuretic, antidiabetic, anti-inflammatory and molluscicidal (Abdelgaleil, S.A.M. et al., 2011; Ahmed and Khater, 2001; Saeed et al., 2015). Damsin (DMS) and neoambrosin (NMS) are the major constituents of its extract (Abdelgaleil, S.A.M. et al., 2011; Saeed et al., 2015). Their anticancer activities were exhaustively deciphered in many studies (Dorskotch and Hufford, 1969; Saeed et al., 2015; Villagomez et al., 2013). However, no previous study has verified the efficacy of damsisa's constituents in alleviation of RA, although damsin and neoambrosin inhibited main inflammatory markers involved in cancer pathogenesis, e.g. NF-k β , STAT, TNF- α (Svensson et al., 2018a; Villagomez et al., 2014; Villagomez et al., 2015; Villagomez et al., 2013). Hereto, the efficacy of damsin and neoambrosin against RA would be assessed. Moreover, their molecular targets are to be identified, especially the key players in RA pathophysiology.

Researchers postulated the pathophysiology beyond RA is the dysregulated persistent production of the major proinflammatory cytokines levels namely; interleukin-1, -6 (IL-1, -6) and tumor necrosis factor (TNF- α) that are directly involved in the joint destruction and inflammation (Aletaha and Smolen, 2018). TNF- α binds to its respective receptor to implement the inflammatory cascade in RA, via enhancing nuclear factor-kappa β (NF-k β). NF-k β is considered as a masterpiece of inflammatory process and immune response in animal models as well the diseased patients. NF-k β plays a central role in pathophysiology of rheumatoid arthritis (Makarov, 2001; Simmonds and Foxwell, 2008) where activated NF-k β is released from the cytoplasmic complex by phosphorylation and proteolytic degradation of the I κ - β subunit. The activated factor gets translocated to the nucleus, and in turn regulates the transcription of target genes of various inflammatory cytokines, such as IL-6, TNF- α , MCP-1 (Ly β et al., 1998). Noteworthy, there is crosstalk between NF-k β , TNF- α and IL-6 which guarantees dissemination and propagation of the inflammatory process with further recruitment of immune cells.

Concomitantly, IL-6 evoked as a promising target for the treatment of RA and this is confirmed by using IL-6 targeting therapy; Tocilizumab. Through its receptor, IL-6 positively regulates inflammation via activation of STAT3, JAK/PI3K/Akt and Ras/Extracellular signal-regulated kinase 1/2 (ERK1/2) pathways (Yoshida and Tanaka, 2014). *In vivo* and *in vitro* studies demonstrated the involvement of PI3K/Akt signaling in the inflamed synovial tissue and immune cells recruitment (Malemud, 2015). In parallel, ERK1/2 is regarded as a regulator of IL-1, -6 and TNF-production and as a transducer for their actions. Moreover, ERK1/2 promotes pannus formation in RA (Thalhammer et al., 2008). Alongside, innate immunity and cytokine production are mediated by toll-like receptors in RA, and several studies showed NF-k β and GSK3 β as the ultimate downstream proteins of the toll-like receptors signaling (Martin et al., 2005).

Inflammatory milieu and immune cells were perpetuated in RA

pathogenesis by expression of the proinflammatory cytokine; cysteine-rich 61 (CCN1/Cyr61) and the chemokine; monocyte chemoattractant protein-1 (MCP-1/CCL2) under TNF- α stimulation. Both are heparin-binding proteins where Cyr61 is a prototypic member of growth regulators named CCN family and participates in neutrophils infiltration and synovial tissue proliferation in RA patients (Haas et al., 2006). On the other hand, MCP-1 regulates the migration and infiltration of monocytes at the inflamed joints, a prominent feature of RA. MCP-1 is highly upregulated even before the onset of RA (Gong et al., 1997; Rantapää-Dahlqvist et al., 2007). Therefore, curbing of these RA inflammatory markers is crucial to break the vicious cycle of inflammatory events in RA.

As on date, no data present about the potential impact of DSM and NMS in treatment of RA disability and its respective signal transduction which represents a promising avenue for therapeutic intervention in this chronic inflammatory disease. To achieve this aim, complete Freund's adjuvant (CFA)-induced arthritis model was used as a model of chronic polyarthritis that sensitizes the immune system to simulate the same clinical and pathological features of RA. Herein, the current study aimed to explore the possible anti-arthritic effect of DSM and NMS against CFA-induced RA in rats and their ability to restore the joint functionality.

2. Material and methods

2.1. Plant material

Aerial parts of *A. maritima* L. were collected from the Botanical Garden of Faculty of Pharmacy, Cairo University. Samples were authenticated by Prof. Dr. Wafaa M. Amer, Botany Department, Faculty of Science, Cairo University. A voucher specimen was deposited in Cairo University herbarium (CAI). *A. maritima* L., the plant list (<http://www.theplantlist.org>), last access, 30 January 2020. Aerial parts were collected and shade-dried in air. Plant material was grinded coarsely.

2.1.1. Extraction and isolation of neoambrosin and damsin

Air-dried aerial parts of *A. maritima* (5 kg) were macerated for 2 days in 70% ethanol (1:5, powder/solvent). The filtrate was evaporated under vacuum at 40 °C. Extraction were repeated six times to yield an extract (750g). The alcoholic residue (600 g) was suspended in water and defatted exhaustively by extraction with petroleum ether (10 \times 200 ml); it yielded 80 g. The defatted extract was extracted with dichloromethane (DCM) (10 \times 250 ml) to yield 160 g DCM extract. A part of the DCM extract (110g) was fractionated using VLC (400g silica, 15 \times 8 cm) starting from pet. ether, DCM in 10% increments in pet.ether till 100% DCM, then increasing polarity using EtOAc in 10% increment in DMC till 100% EtOAc. Fractions were concentrated and monitored by TLC and similar fractions were pooled together. Neoambrosin was isolated by repeated column chromatography using 7–10 % EtOAc/pet.ether. It was crystallized from DCM to give colorless radiating needles (850 mg).

Damsin was eluted at 15–20 % EtOAc/pet.ether. It was crystallized from DCM to give colorless rosette needles (1050 mg).

2.1.2. HPLC test for purity

HPLC Agilent 1200 infinity instrument was armed with manual injector and DAD detector. The mobile phase system consisted of solvent A & B, water containing 0.1% formic acid and acetonitrile, respectively. The separation was in gradient mode and started by using solvent B at 43% for 2 min, then, it was gradually increased to attain 75% at 34 min then increased to 100% at 36 min. Afterwards the column was washed using 100 % acetonitrile for 2 min. Detection wavelengths were set at 220 and 240 nm. The purity of neoambrosin and damsin were confirmed by HPLC analysis (Fig. 1a and b).

2.1.3. Identification and structure elucidation of neoambrosin (1) and damsin (2)

Two compounds 1 and 2 were purified and identified from DCM fraction and comparison with authentic samples and by NMR analysis. Neoambrosin (1) was obtained as colorless radiating needles. Its structure was established by NMR. The ^{13}C NMR spectrum revealed 15 signals. Two methyl groups (^1H , ^{13}C -NMR) (δ 1.15/14.94, δ 1.169/21.12), CH₂ groups including one olefinic [δ (1.65, 1.81)/30.12, δ (1.96, 2.12)/23.97, δ (2.76, 3.22)/38.75, (δ 5.5, 6.2)/119.87], CH groups including one olefinic (δ 2.91/39.91, δ 3.37/43.47 δ 4.41/79.79, δ 6.24/124.32), and quaternary carbons (δ 58.46, 138.8, 149.27, 169.83, 213.9) supplementary table (S1). These spectral data were suggestive of SLs. The skeleton and the relative configuration of the pseudoguaianolide was compatible with literature values from previous studies (Abdelgaleil, S. et al., 2011).

Damsin (2) was isolated as colorless rosette needles Its ^{13}C NMR

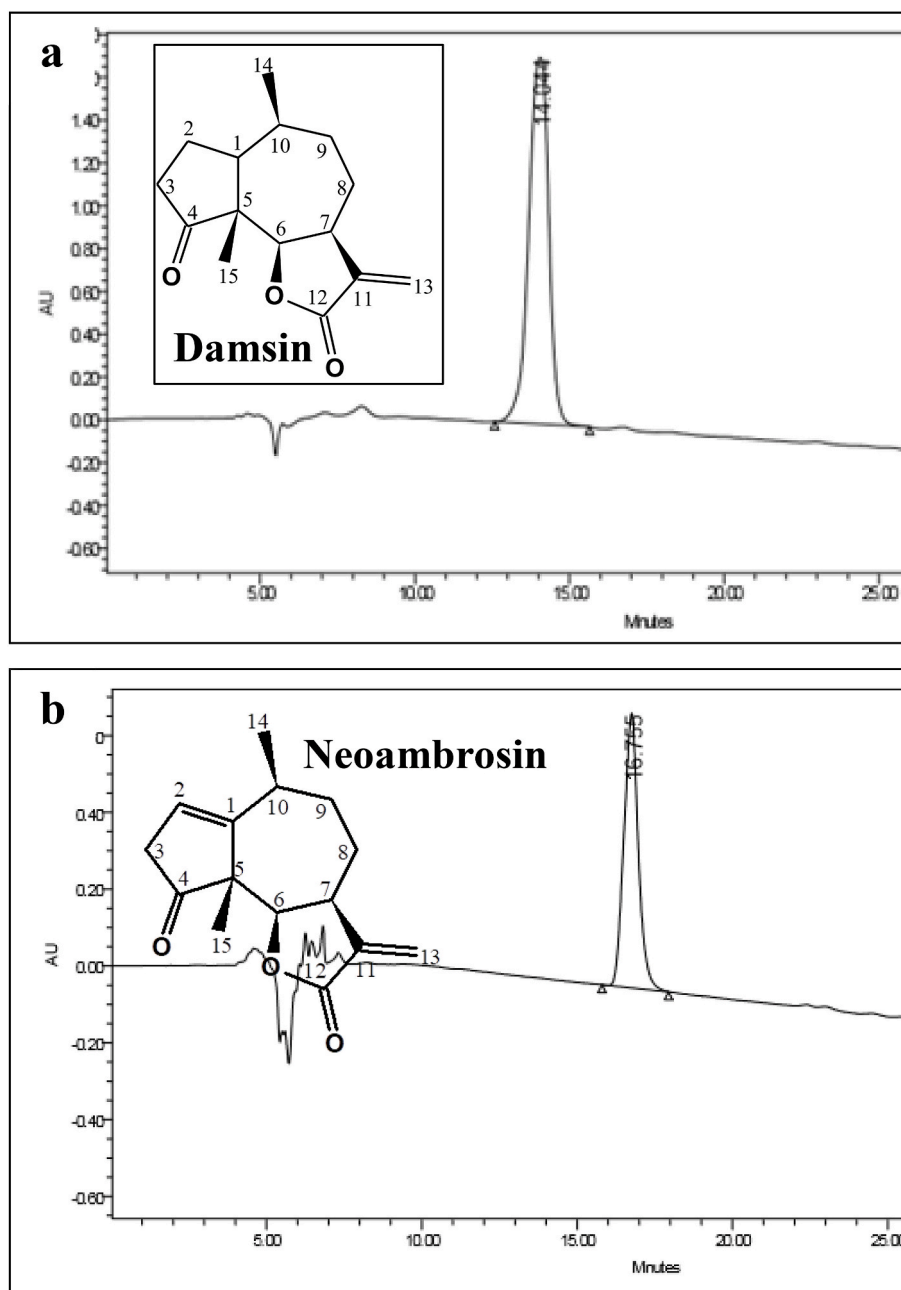


Fig. 1. HPLC chromatograms of pure isolated damsin (a), and neoambrosin (b). The inserts contain the chemical structures.

spectra also contained 15 signals with the lack of two olefinic resonances. There is two CH₃ groups (δ 0.990/13.73, δ 0.995/15.83), five CH₂ groups including one olefinic exo-methylene (δ 1.64, 1.83/33.33, δ 1.80, 2.01/24.1, δ 1.80, 2.01/25.64 δ 2.24, 2.4/36.1, δ 5.58, 6.17/120.79), four CH groups (δ 2.20/34.22, δ 2.01/45.32, δ 3.2/44.32 δ 4.47/81.74) and four quaternary carbons (δ 54.85, 139.65, 170.23, 218.99) were identified. The data conforms to the literature (Abdelgaleil, S. et al., 2011).

Chemical shifts of ¹H-NMR and ¹³C-NMR of neoambrosin & damsine are shown in Table 1.

2.2. Animals

Adult male Wistar rats (8–10 weeks), weighing 140–190g, obtained from the animal facility of Faculty of Pharmacy, Cairo University, Egypt. Animals were kept under controlled environmental conditions: constant temperature (25 °C \pm 2 °C), humidity (60% \pm 10%) and a 12/12-h light/dark cycle and they were allowed to acclimatize for one week prior to the study. Standard chow diet and water will be allowed ad libitum. The study was approved by the Ethics research committee of Faculty of Pharmacy, Cairo University [Approval number: MP(2245)], and in accordance with the Guide for the Care and Use of Laboratory Animals published by the US National Institutes of Health (NIH Publication No 85–23, revised 2011). All rats were gently treated, where squeezing, pressure, and tough handling were avoided as well a sample size power analysis (power = 0.8, α = 0.05) (Li et al., 2018) was performed to reduce the number of animals used.

2.3. CFA-induced arthritis

CFA (0.1 ml) was injected in the right hind paw while the contralateral left paw received saline (0.1 ml) and served as a control (Pearson,

Table 1
Chemical shifts of ¹H-NMR and ¹³C-NMR of Neoambrosin & Damsine.

Number	¹ H-NMR (400 MHz, CDCl ₃)	¹³ C-NMR (100 MHz, CDCl ₃)	¹ H-NMR (400 MHz, CDCl ₃)	¹³ C-NMR (100 MHz, CDCl ₃)
1	–	149.27	2.177 (1H, m, H-1)	45.99
2	5.95 (1H, t, J = 2.12 Hz, H-2)	124.32	1.93 (1H, m, H-2)	23.91
3	3.15 (1H, dd, J = 1.88 Hz, H-3a) 2.81 (1H, dd, J = 2.44 Hz, H-3b)	39.91	2.38 (1H, ddd, J = 1.32, 9.9, 1.4 Hz, H-3)	36.10
4	–	213.9	–	218.99
5	–	58.46	–	54.85
6	4.41 (1H, d, J = 8.8 Hz, H-6)	79.79	4.47 (1H, d, J = 8.68 Hz, H-6)	81.74
7	3.37 (1H, m, H-7)	43.47	3.26 (1H, m, H-7)	44.32
8	2.05 (2H, m, H-8a,b)	23.97	1.8 (2H, m, H-8)	25.64
9	1.78 (2H, m, H-9a,b)	30.12	1.78 (2H, m, H-9)	33.33
10	2.89 (1H, m, H-10)	38.75	2.44 (1H, m, H-10)	34.22
11	–	138.82	–	139.65
12	–	169.83	–	170.23
13	6.24 (1H, d, J = 3.6 Hz, H-13a) 5.51 (1H, d, J = 3.32 Hz, H-13b)	119.87	6.17 (1H, d, J = 3.2 Hz, H-13a) 5.48 (1H, d, J = 2.84 Hz, H-13b)	120.79
14	1.15 (3H, d, J = 7.4 Hz, H-14)	21.12	0.990 (3H, d, J = 7.4 Hz, H-14)	15.83
15	1.17 (3H, s, H-15)	14.94	0.995 (3H, s, H-15)	13.73

1964). After 1 week, the right hind paw received the 2nd dose of CFA (0.1 ml) to enhance 2^{ry} arthritis. After 14 days, the inflammation was established and furthermore confirmed by measuring the volume of paw by using Plethysmometer (Ugo Basile 7140) to establish the model.

2.3.1. Experimental design

Forty rats were randomly allocated using a computer-generated randomization table into 4 groups (n = 10 for each group). The study was conducted for 28 days starting from the 1st injection of CFA. The groups were as following; normal group (NRML), CFA-induced arthritis group (CFA), CFA-induced arthritis treated with damsine (DMS) (10 mg/kg, i.p.) and CFA-induced arthritis treated with neoambrosin (NMS) (10 mg/kg, i.p.). DMA and NMS were dissolved in saline containing 0.1 % Tween 80; this vehicle was utilized for the daily injection of the control group. The treatments; NMS and DMS were injected on the 14th day of CFA injection and continued till the 28th day. After establishment of arthritis, rats were subjected to five behavioral assessments in the following orders; paw volumes, knee joint diameters, spontaneous locomotor activity, cold allodynia and finally analgesymeter as stated in Fig. 2. Tests were performed with 2 h resting period between the tests. Paw volumes and knee joint diameters were assessed as indices of inflammation using Plethysmometer (Ugo Basile 7140) and digital electronic calipers (Mitutoyo, UK), respectively. The paw volumes were expressed in milliliters as difference between the right and left paws. Quantification of “pain-like” behaviors was done by 2 behavioral methods. The first method was stimulus-evoked nociception that was measured by recording the paw withdrawal latency in cold allodynia (hind paw subjected to cold water stimuli at 4.5 °C) and analgesymeter (Ugo Basile). The second non-stimulus evoked (spontaneous) nociception was assessed by recording the distance travelled and immobility time. Meanwhile, they are measures of locomotor activity in open-field arena (80 × 80 × 40 cm). Open-field arena was equipped with a computer interface and ANY-Maze video tracking software (Stoelting Co, USA) (Deuis et al., 2017). Concomitantly, the body weight of rats was recorded. All measures were performed on days 0, 14, 17, 20, 23, 26 and 28 except locomotor analysis was assessed on day 28. After the behavioral tests, blood samples for serum separation were withdrawn from retro-orbital plexus under thiopental then the animals were euthanized. Following sacrifice, the removed hind paws were divided into subsets, first subset (n = 3) for histopathological assessment. The second subset (n = 7) was subjected to snap freezing before storage in -80 °C freezer until assessing biochemical parameters using different techniques; enzyme-Linked Immunosorbent Assay (ELISA), western blotting and quantitative real time PCR (qRT-PCR).

2.3.2. Histopathological examination

Dissected paws samples were fixed in 10% neutral buffered formalin for 72 h. Then samples were decalcified by using (Cal-X II, Fisher Scientific) for 25 days then processed in serial dilutions of ethanol and cleared in xylene then embedded in synthetic wax paraplast tissue embedding medium. 5 μ m thick tissue sections were cut by rotatory microtome and fixed to glass slides, tissue sections were stained by Hematoxyline and Eosin as a general examination staining method. Tissue sections were assessed for abnormal morphological changes and scored according to Saad et al. (2019) by using Full HD microscopic imaging system (Leica Microsystems GmbH, Germany). All standard procedures for samples processing and staining as outlined by Drury and Wallington (1983).

2.3.3. Enzyme-linked immunosorbent assays

Using rat-specific enzyme-linked immunosorbent assay (ELISA) kits and according to the manufacturer's instructions, the following parameters were determined; CCN1 (MyBiosource, San Diego, USA, Cat. No: MBS915153), NF- κ B p65 (MyBiosource, San Diego, USA, Cat.No: MBS015549), IL-6 (MyBiosource, San Diego, USA, Cat.No: MBS726707), TNF- α (MyBiosource, San Diego, USA, Cat.No:

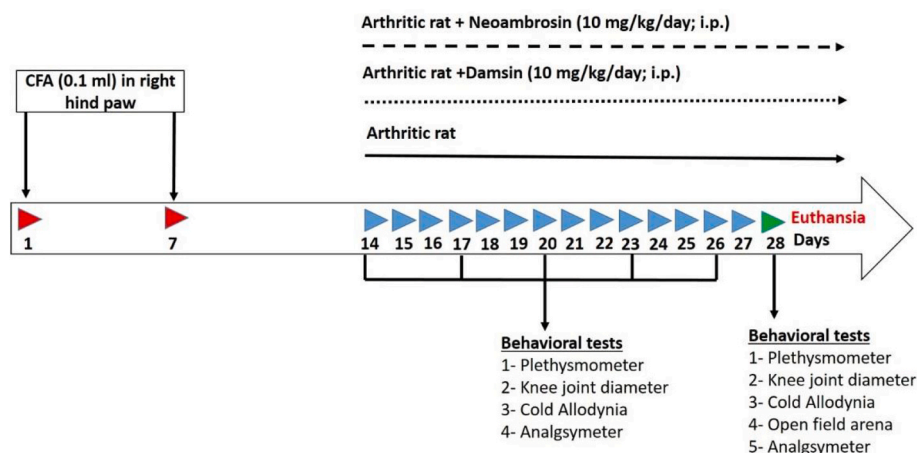


Fig. 2. Time schedule for DMS and NMS with behavioral assessments in arthritic rat model.

MBS355371). The results were expressed as picogram per milliliter serum for CCN1, NF- κ B, p65, IL-6 and TNF- α .

2.3.4. Quantitative real-time-PCR (qRT-PCR)

Tissues from all different groups were homogenized and total RNA was extracted with RNA easy Mini Kit (Qiagen) then the purity of produced RNA was assessed by Beckman dual spectrophotometer (USA). Afterwards, reverse transcription of extracted RNA was done utilizing high capacity cDNA Reverse Transcriptase kit (Applied Biosystem, USA). The amplification of cDNA was subsequently done by the Syber Green I PCR Master Kit (Fermentas) using the Step One instrument (Applied Biosystem, USA). Briefly, 5 μ l of cDNA were mixed with 12.5 μ l SYBR Green mixture, 5.5 μ l RNase free water and 2 μ l of each primer in a 25 μ l reaction volume. The conditions of amplification step included 10 min at 95 $^{\circ}$ C for activation of AmpliTaq Gold DNA polymerase, followed by 40 cycles at 95 $^{\circ}$ C for 15 s (denaturing) and 60 $^{\circ}$ C for 1 min (annealing/extension). Normalization for the expression of each target gene was referred to the mean critical threshold (CT) values of β -actin house-keeping gene expression using the $\Delta\Delta$ Ct method (Livak and Schmittgen, 2001). Primer sequence for MCP1 and β -actin gene was presented in Table 2.

2.3.5. Western blotting

Ice cold supernatants of homogenized tissues were lysed in RIPA buffer (50 mM Tris HCl pH 8, 150 mM NaCl, 1% Triton X-100, 0.5% sodium deoxycholate and 0.1% SDS) provided with phosphatase inhibitor cocktail. After centrifugation and protein determination by BCA protein assay kit (Thermo Fisher Scientific Inc., USA), 7.5 μ g protein of each sample was boiled with Laemmli buffer at 95 $^{\circ}$ C for 5 min to ensure denaturation. After protein extraction, equal amounts of protein loaded on sodium dodecyl sulfate polyacrylamide gel electrophoresis (SDS-PAGE), transferred to an Immobilon membrane (Millipore) followed by blocking 5% bovine serum albumin (BSA). The blot was incubated on a roller shaker overnight at 4 $^{\circ}$ C with either p(Ser473)-Akt (Boster Biological Tech., Pleasanton, CA, USA, Cat No: P00024-5), p(Ser9)-GSK3 β (GeneTex, Alton Pkwy Irvine, CA, USA, Cat No: GTX59576), p(Thr202/Tyr204)-ERK (Biovision, Milpitas, CA, USA, Cat No: A1589-100), p(Tyr705)-STAT3 mouse anti-rat (Santa Cruz Biotechnology, Heidelberg,

Table 2

Primer sequence used for RT-PCR.

mRNA species	Primer sequence (5'-3')
β -actin	F: 5'-CTAAGCCAACCGTAAAAAG-3'
	R: 5'-GCCTGGATGGCTACGTACA-3'
MCP-1	F: 5'-AGCATCCACGTGCTGTCTC-3'
	R: 5'-GATCATCTTGCAGTGAATGAG-3'

Germany, Cat. No: sc-8059). Afterwards, secondary antibodies (1:1000 dilution) were incubated for 2 h at room temperature. Densitometric analysis of the immunoblots was performed to quantify the amounts of protein by Image analysis software on the ChemiDoc MP imaging system (version 3) produced by Bio-Rad (Hercules, CA). Data are represented as arbitrary units (AU) after normalization for β -actin protein expression.

2.3.6. Statistical analysis

All data were presented as mean \pm S.D. Results were analyzed using one-way analysis of variance test (one-way ANOVA) followed by Tukey's multiple comparison test for all parameters. Moreover, Pearson's correlation analysis was used to evaluate the relationship between locomotion activity with arthritis signs and stimulus-evoked pain like behavior. Statistical analysis was performed using Graph Pad Prism software version 8 (San Diego, CA, USA). For all statistical tests, the level of significance was fixed at $p < 0.05$.

3. Results

3.1. Effect of DSM and NMS on non-stimulus evoked and stimulus-evoked pain-like behaviors of CFA-induced arthritis

Rheumatoid arthritis is a disabling disease with chronic pain that affects the locomotion of the affected subjects. The pain-like behavior was reflected on the locomotor activity as a measure of spontaneous evoked pain where CFA injection lowered the distance travelled and prolonged immobility time to reach 7.6 % and 3-fold that of CFA-untreated animals, respectively. Herein, DSM and NMS evoked the rats' locomotion by increasing the distance travelled to 7.19 and 6.75-folds as well shortened immobility time by 36.7 and 30 % respectively compared to rats with inflamed paws (Fig. 3a and b). In mechanical evoked pain, CFA rats from the 14th day showed a significant decrease in pain threshold till the 28th day compared to CFA-untreated group. The time of paw withdrawal was shortened from the 14th day post-CFA administration till the end of experiment as compared to saline-treated rats while DSM and NMS increased the arthritic rats' tolerability starting from the 20th day till the day of sacrifice (Fig. 3c). DSM and NMS counteracted CFA-induced pain starting from the 20th day and specifically DSM enabled rats to tolerate the pain of larger weights to be as normal group on 26 and 28th days (Fig. 3d).

3.2. Effect of DSM and NMS on body weight and arthritis features of CFA-induced arthritis

One of the parameters that assess the progression of disease is measuring body weights beside hind paw volume and knee joint

Open Field Test

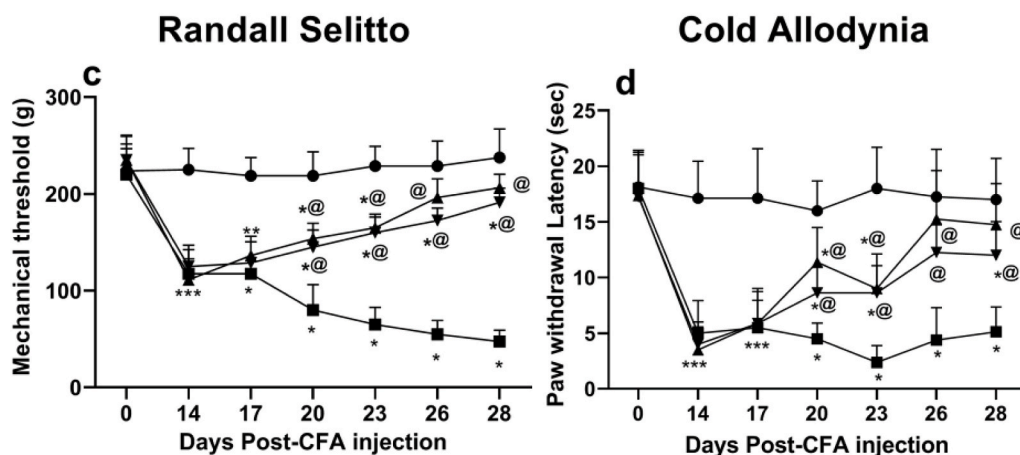
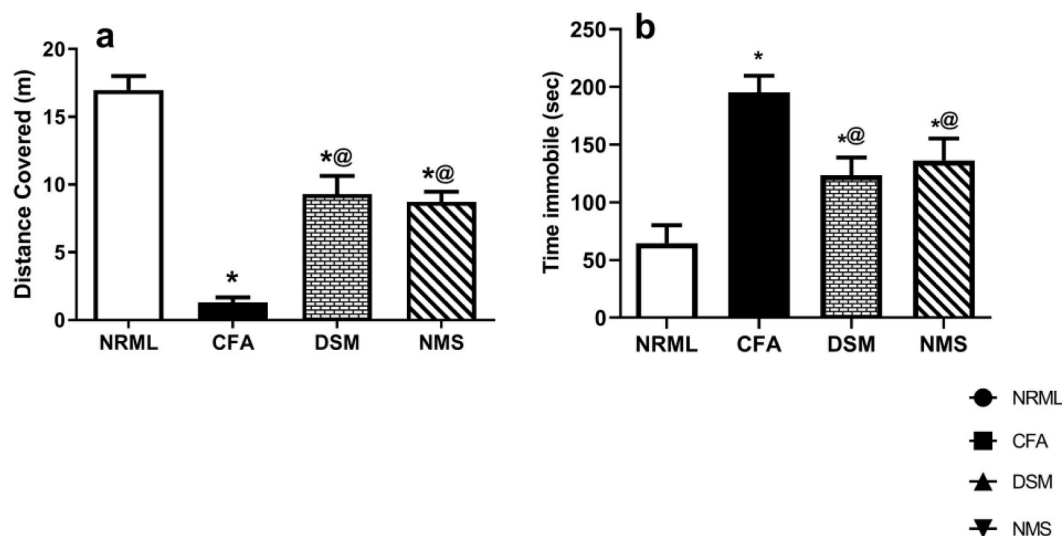


Fig. 3. Effect of DSM and NMS on non-stimulus evoked and stimulus-evoked pain-like behaviors of CFA-induced arthritis. Each bar with vertical line represents mean \pm S.D. of 10 rats per group. * vs control, @ vs CFA, # vs DSM using one-way ANOVA followed by Tukey's post hoc test; $p < 0.05$. CFA; Complete Freund's adjuvant, DSM; dapsin, NMS; neoambrosin.

diameter. Body weight was significantly affected in arthritic group compared to normal animals and started to decrease after 17 days of CFA injection. This decrease was opposed at the 20th day by DSM and NMS administration till the end of the disease course in respect to the model group (Fig. 4a). Meanwhile, joint knee diameter and hind paw volume were continued to increase significantly with CFA from 14th day. However, these alterations were lowered by concurrent administration of either DSM or NMS in CFA rats that show significance starting from the 23th day (Fig. 4b and c). To assess disability of treated and untreated rats, the present study correlated between distances travelled as a measure of locomotion with arthritis signs as well stimulus-evoked pain behavior as in Table 3. It is concluded that there is a negative correlation between distances travelled with inflamed paw ($r = -0.9002$, $p < 0.0001$) and joint diameter ($r = -0.8364$, $p < 0.0001$) where CFA rats showing swollen paw or joint during arthritic disease travelled a significantly shorter distance. On contrary, normal, DSM and NMS rats

with smaller paw and joint alongside travelled longer distance. The positive correlation was found between locomotion with pain tolerability ($r = 0.8775$, $r = 0.7853$, $p < 0.0001$) where CFA-induced pain disabled locomotion while DSM and NMS suppressed pain enhanced locomotor activity.

3.3. Effect of DSM and NMS on the histopathological examination of the rat hind paw

Histopathological examination of the rat hind paw was presented in Fig. 5. In NRML animals, there was normal morphological appearance of epidermal layer (red star) with intact keratinocytes as well as intact dermis (black star) with normally mature collagen fibers and connective tissue cellular elements with minimal inflammatory cells records (Fig. 5a). Also in subcutaneous tissues, it is observed normally loosely arranged thin collagen and elastic fibers with abundant fibroblasts, few

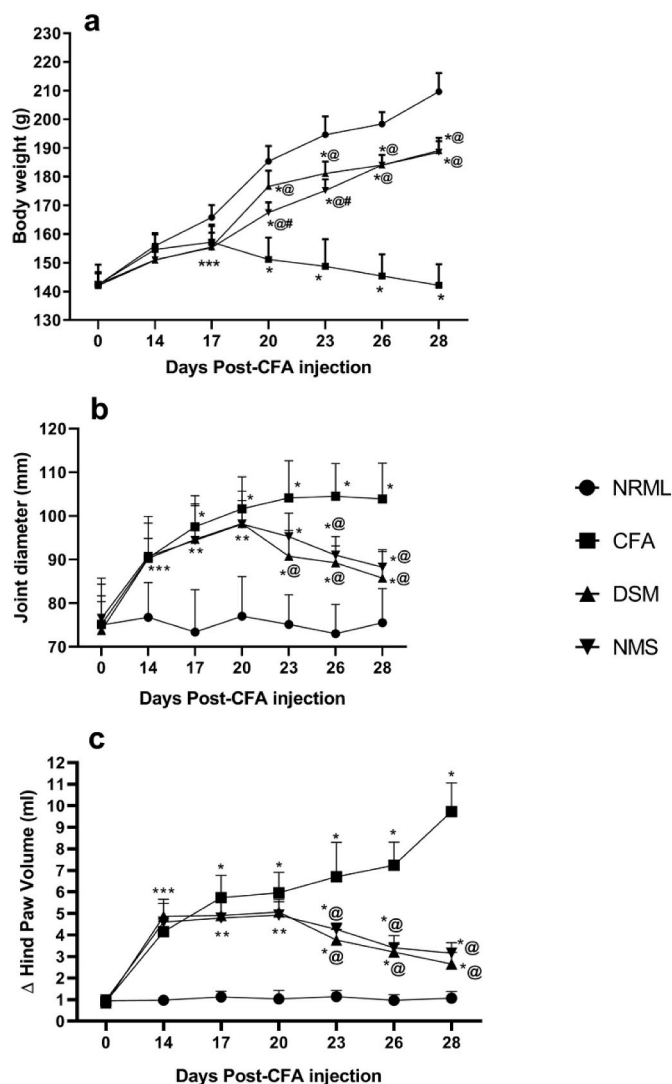


Fig. 4. Effect of DSM and NMS on body weight and arthritis signs of CFA-induced arthritis (5a, b,c). Each bar with vertical line represents mean \pm S.D. of 10 rats per group. * vs control, @ vs CFA, # vs DSM using one-way ANOVA followed by Tukey's post hoc test; $p < 0.05$. CFA; Complete Freund's adjuvant, DSM; damsine, NMS; neoambrosin.

Table 3

Correlation coefficient (r) between locomotion activity with arthritis signs and stimulus-evoked pain like behavior.

	Paw volume (ml)	Joint diameter (mm)	Mechanical threshold (g)	Paw withdrawal latency (sec)
Distance travelled (m)	$r = -0.9002^{***}$ $p < 0.0001$	$r = -0.8364^{***}$ $p < 0.0001$	$r = 0.8775^{***}$ $p < 0.0001$	$r = 0.7853^{***}$ $p < 0.0001$

Correlation was done on all investigated rats ($n = 40$) using Pearson's correlation with significance at $p < 0.05$.

scattered fatty cells and minimal records of inflammatory cells infiltrates as shown in Fig. 5b. Together, there was a normal histological structure of articular hyaline cartilages from different joints with intact smooth articular surfaces, showing higher density of intact chondrocytes (yellow arrow) at different cartilaginous zones (Fig. 5c). On the contrary, rats with CFA-induced arthritis showed severe dermatitis with marked increase of epidermal thickening, degenerative changes of basal cell layer (red star) and many hemorrhagic zones at dermoepidermal

junction (arrow) with severe inflammatory cells infiltrations in dermal layer (dashed arrow) (Fig. 5d). Concurrently, severe subcutaneous inflammatory cells infiltration (star) from different populations as well as many congested and dilated subcutaneous blood vessels (arrow) were observed as presented in Fig. 5e. All these CFA-induced alterations were accompanied with many articular surfaces irregularities, erosion and notches (black arrows) coupled with marked reduction of numbers of chondrocytes and higher records of degenerated pyknotic chondrocytes (dashed arrow) (Fig. 5f). After 14 days of treating arthritic rats with DSM, the microscopic examination showed organized morphological features of epidermis (red star) as well as dermis (black star) without records of structural abnormalities. Concerning subcutaneous tissue, DSM-treated rats showed almost intact subcutaneous connective tissue without abnormal morphological changes and minimal records of inflammatory cells infiltrates. This was confirmed with organized morphological features of articular cartilages with higher density of apparent intact chondrocytes with fewer degenerated cells (dashed arrow) and smooth articular surfaces (Fig. 5g, h & i). Animals injected with NMS showed almost intact epidermal layer with normal thickness (red star) and mild inflammatory cells infiltrates in dermal layer (dashed arrow). However, NMS treatment showed persistence of abundant inflammatory cells infiltrates (star) with minimal records of congested blood vessels. Regarding the articular cartilage, samples demonstrated fewer records of articular surface erosion (black arrows) as well as numbers of degenerated pyknotic chondrocytes (dashed arrow). However; higher density of chondrocytes were observed at different zones of articular surfaces. (Fig. 5j, k & l). The histopathological scores were presented in Table 4.

3.4. Effect of DSM and NMS on inflammatory alterations in arthritic rat hind paw

The inflammatory cytokines are stimulators of inflammation. Notably, CFA group exhibited marked elevation in p65-NF- κ B, TNF- α and IL-6 and levels to reach 9.58-, 8.85-, 9- and 4.14-folds compared to CFA-free rats. Surprisingly, DSM showed significant anti-inflammatory effect via lowering p65-NF- κ B, TNF- α , IL-6 levels by 86, 71.38 and 64 % compared to arthritic group. Similar findings were observed in NMS-treated rats where the previous inflammatory cytokines in the same order were lowered to reach 20, 46 and 56 %; respectively of the CFA group (Fig. 6a, b, c).

3.5. Effect of DSM and NMS on proinflammatory cytokine Cyr61 level and gene expression of MCP-1 in arthritic rat hind paw

This study demonstrated significant increase in level of Cyr61 and gene expression of MCP-1 in arthritic rats to reach 6.76- and 10.8-folds of the normal animals. Post-treatment with DSM and NMS effectively counteracted these effects, as manifested by the decrease of Cyr61 by 80, 58 % and MCP-1 by 68, 55 %. This is accompanied by effectiveness of DMS in lowering Cyr61 and MCP-1 over NMS by 29, 52 % (Fig. 6d and e).

3.6. Effect of DSM and NMS on phosphorylation of downstream signaling cascade proteins in arthritic rat hind paw

Survival pathway showed significant role in establishing inflammatory process. The progression of inflammation requires phosphorylation of the upstream mediator Akt, GSK3 β , ERK1/2 and STAT3. Injection of rats with CFA showed substantial increase in phosphorylation of Akt, ERK1/2 and STAT3 by 4, 2.65 and 1.8-folds of normal animals while decreased inactivation of active GSK3 β by 68%. On the contrary, DSM suppressed CFA-induced phosphorylation to reach 26, 38 and 40 % in respect to Akt, ERK1/2 and STAT3 and enhanced that of GSK3 β to reach 16-fold of arthritis group. Concomitantly in the same order, NMS impeded the phosphorylation of survival pathway to lower to 42, 65 and

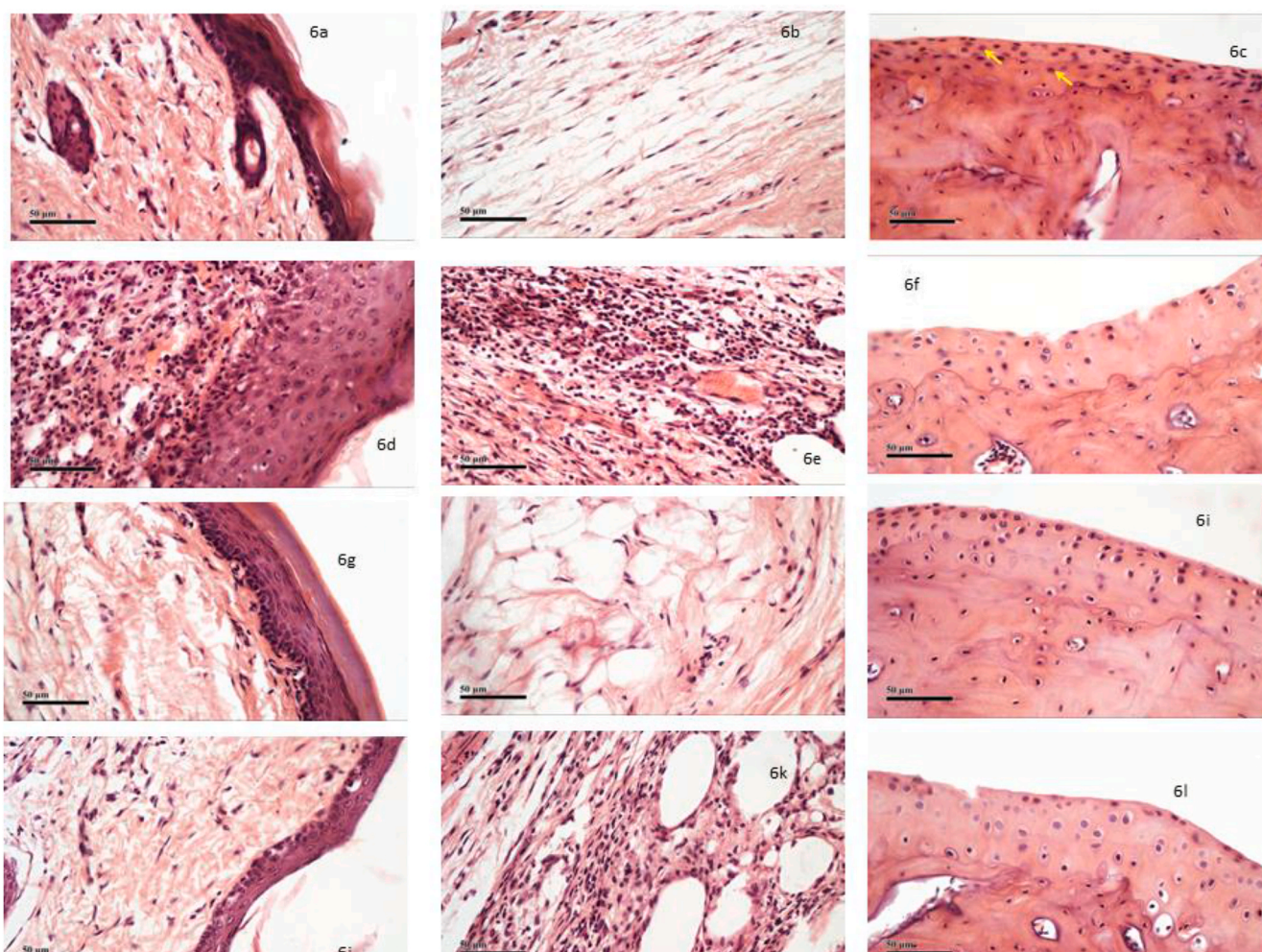


Fig. 5. Effect of DSM and NMS on histopathological alterations induced in CFA-induced arthritis. Representative photomicrographs of H & E stain of different sections of rat hind paw; epidermal, dermis, subcutaneous tissues and articular cartilage. **a-c** normal group, **d-f** CFA group, **g-i** DSM-treated group and **j-l** NMS-treated group. Magnification: x400 CFA; Complete Freund's adjuvant, DSM; damsine, NMS; neoambrosin.

Table 4
Effect of DSM and NMS on histopathological scoring of hind paws perturbations.

Histopathological perturbations	Groups			
	NRML	CFA	DSM	NMS
Epidermis and dermis				
Epidermal lesions	-	+++	-	+
Dermal inflammatory cells	-	+++	-	+
Subcutaneous				
Inflammatory cells	-	+++	+	+++
Blood vessels congestion	-	++	-	+
Articular cartilage				
Surface erosions	-	+++	-	++

- Nil, + mild, ++ moderate, +++ severe, CFA; Complete Freund's adjuvant, DSM; damsine, NMS; neoambrosin.

60 % compared to arthritic animals that subsequently raised phosphorylated GSK3 β by 4.5-folds. The superiority of DMS in repressing the phosphorylated forms of survival pathway was witnessed in Akt, ERK1/2 and STAT3 parameter which were lower by 61, 57 and 33 % (Fig. 7a, b, d) that confirmed with elevated p-GSK3 β to reach 2.9-folds in respect to NMS-treated animals (Fig. 7c).

4. Discussion

The study explored the efficacy of 2 pseudoguaianolide

sesquiterpene lactones (SL) compounds as promising molecules that improved RA cardinal features; function, pain and inflammation of joints in an animal model of CFA-induced arthritis. This notion was supported by several array of evidence; (i) reduction of enlarged joint diameter and paw volume accompanied by improvement of locomotor activity and pain sensitivity; (ii) inhibition of Akt, NF-k β , GSK3 β and STAT3 signaling; (iii) suppression of inflammatory cytokines; IL-6 and TNF- α ; (iv) impeding of immune cell migration via inhibiting MCP-1 and Cyr61. All these assessments were assured in histopathological examinations of rat hind paw.

Efficacies of both DMS and NMS were behaviorally assured through the assessment of edema and hypersensitivity utilizing pethysmometer and withdrawal reflex in response to both mechanical and cold stimuli. Alongside, Arthritis-induced disability in rats was noted through alteration in spontaneous behavior in open field arena that showed decreased distance covered by animals and this was correlated positively with pain tolerability and negatively with arthritic joint. This can be owed to sustained flexion of the knee joint as well as the active movement-induced pain in the inflamed limb (Stein et al., 1988). In the current study, DSM and NMS reversed the enlarged paw volume; knee joint diameter together with intolerable pain stimulus supported this plausible justification. Furthermore, the alteration in rats' body weight was used as a caliber for the efficacy of treatments during the course of the disease. During RA progression in rats, the gain of body weight is slowed and this in line with Granado et al. (2005) who justified such

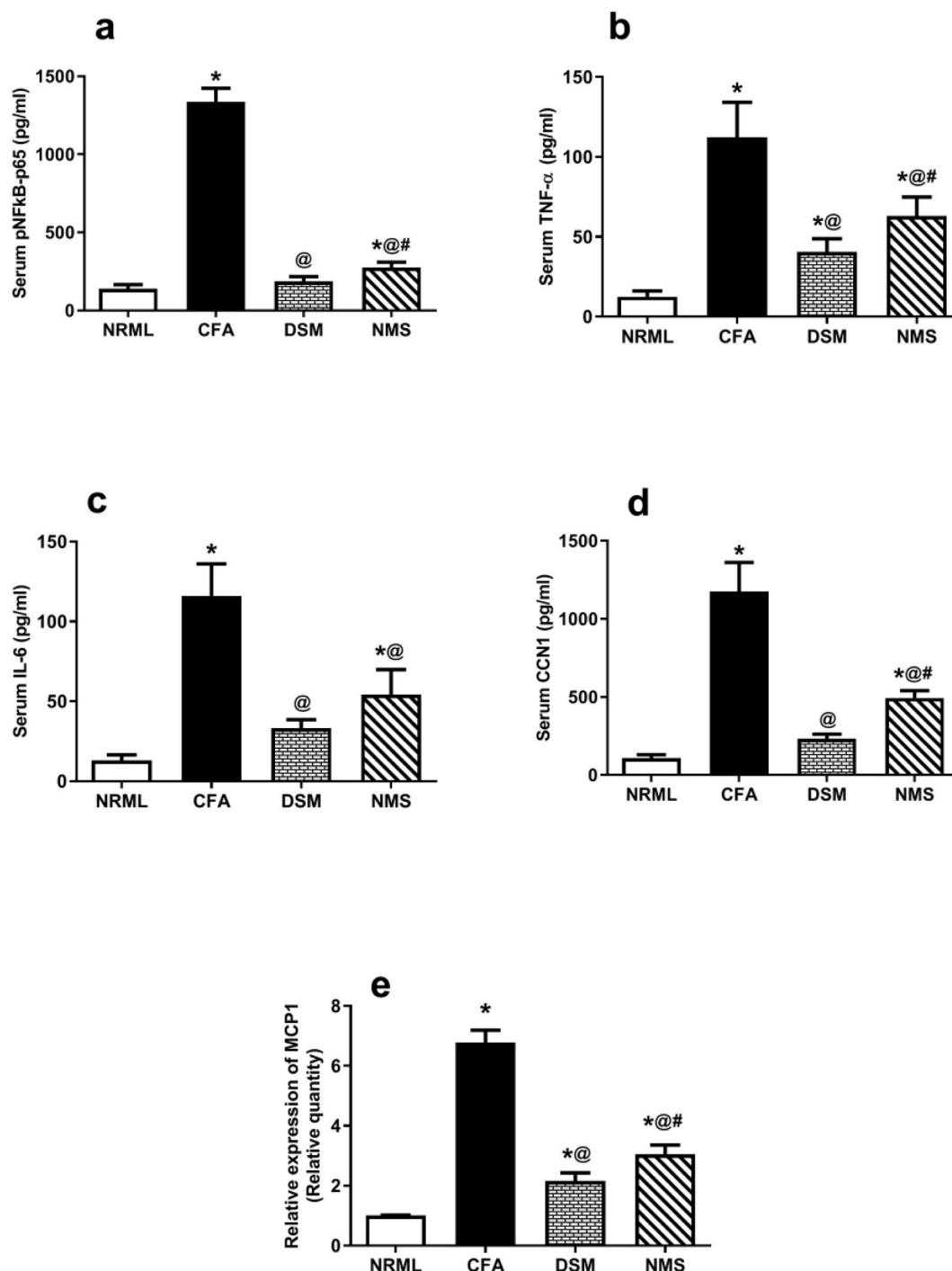


Fig. 6. Effect of DSM and NMS on level of inflammatory markers and chemokine gene expression in CFA-induced arthritis. Each bar with vertical line represents mean \pm S.D. of 6-7 rats per group. * vs control, @ vs CFA, # vs DSM using one-way ANOVA followed by Tukey's post hoc test; $p < 0.05$. CFA; Complete Freund's adjuvant, DSM; damsin, NMS; neoambrosin.

phenomena due to overexpression of TNF- α which induces muscle wasting *via* activating NF- κ B where both were flipped with DSM and NMS.

The plethora of the released inflammatory mediators in CFA model is sufficient to assess anti-arthritic properties of new compounds like SL. The anticancer and anti-proliferative activities of SL in several studies ensure their potentiality to reverse joint proliferation and inflammation particularly, when the targeted proliferating proteins in cancer pathogenesis are the same accused one in the arthritis milieu such as TNF- α , Akt, ERK1/2, NF- κ B, STAT3 and GSK3 β . Moreover, the active moiety of

SL; α -methylene- γ -lactone was demonstrated as potent inhibitor to protein kinase signaling such as Akt, ERK1/2, GSK3 β and their substrates like STAT3 (Schepetkin et al., 2018) and this was substantial in the present study after administration of DSM and NMS in CFA model. Consequently, NF- κ B and its regulatory signaling pathways have become a cogent point for immunomodulation and anti-inflammatory activity. The α -methylene- γ -lactone moiety in SL compounds act as a Michael acceptor and irreversibly alkylate enzymes and transcription factors; NF- κ B and STAT3, causing their inactivation (Ivanescu et al., 2015). In the current study, DSM and NMS blocked NF- κ B in arthritic rat which

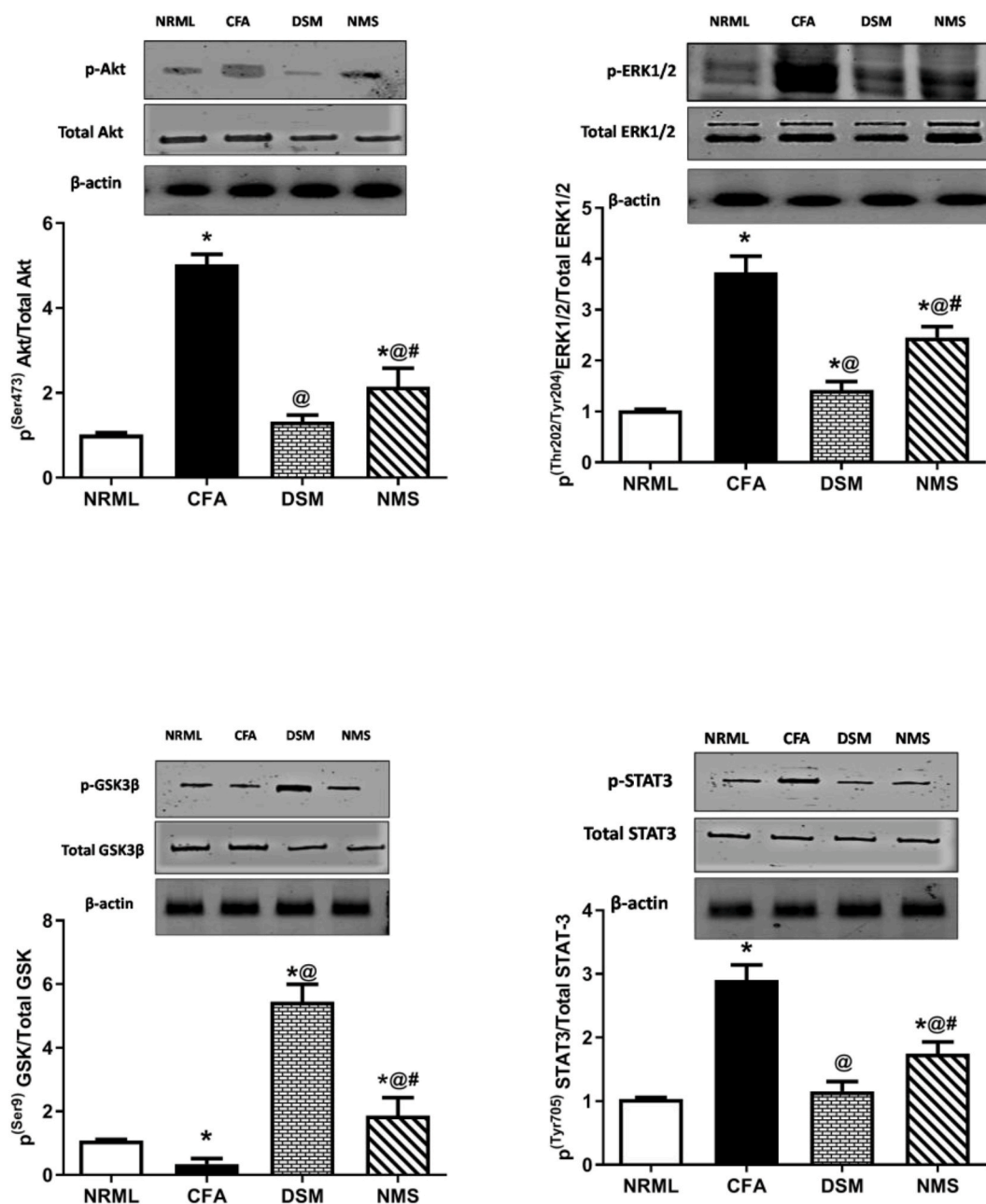


Fig. 7. Effect of DSM and NMS on phosphorylation of downstream signaling cascade proteins in CFA-induced arthritis. Each bar with vertical line represents mean \pm S.D. of 6–7 rats per group. * vs control, @ vs CFA, # vs DSM using one-way ANOVA followed by Tukey's post hoc test; $p < 0.05$. CFA; Complete Freund's adjuvant, DSM; damsine, NMS; neoambrosin.

represents the hub of their anti-inflammatory action. The potency of pseudoguaianolide SL as anti-inflammatory agents was related to the constraint of the NF- κ B (Youl Cho, 2006) indirectly by inhibiting the degradation of I κ B, the inhibitory subunit of NF- κ B (Hehner et al., 1998; Ly β et al., 1998) or directly by interacting with cysteine 38 in the p65/NF- κ B to suppress the interaction between NF- κ B/p65 and DNA (García-Piñeres et al., 2001; García-Piñeres et al., 2004). NF- κ B imprisonment prompted by DSM and NMS ameliorated downstream inflammatory cytokines as verified by the fall of TNF- α homogenate level.

Survival pathway Akt is the proliferating pathway accused for synovial hyperplasia and pannus formation. *In Vitro* and *In Vivo* studies related the synovial hyperplasia to deficiency in upstream inhibitor of Akt/NF- κ B; tumor suppressor phosphatase PTEN (Pap et al., 1999). In the current work, the anti-proliferating activity of DSM and NMS was demonstrated by lowering paw p-Akt that may partly have impact in

limiting the progression of the arthritis induced by CFA in rat model. This may be attributed to direct dephosphorylation of Akt at Ser473 as elaborated by Chin and Toker (2009) or indirect through α -methylene- γ -lactone moiety of this class that covalently represses the focal adhesion kinase; the upstream activator of PI3K/Akt signaling pathway (Berdan et al., 2019). All these studies clarify the potency of SL as anti-proliferating compounds against RA. Together, previous studies linked NF- κ B with Akt signaling where Akt induces transcriptional activity of NF- κ B by inducing phosphorylation and subsequent degradation of inhibitor of kappa B (Ikappa B) (Kane et al., 1999). This intuitively shows NF- κ B may mediate invasiveness of Akt that proliferates and protects rheumatoid synovial fibroblast from Fas-induced apoptosis (García et al., 2010). In the same context, upregulation of PI3K/Akt pathway in synovial cells of RA mediates the proliferating and inflammatory effects of TNF- α (Bartok et al., 2012; Zhang et al., 2001). This

may interpret the anti-proliferating and anti-inflammatory effect of DSM and NMS due to the prohibition of TNF- α /PI3K/Akt/NF- κ B signaling pathway.

The dominant cytokine in the arthritic joint; TNF- α with its downstream proteins; NF- κ B and ERK1/2 weave the pathogenesis of RA (Khansai et al., 2017). Sun et al. (2018) elaborated the crucial inflammatory role of TNF- α in isolated rheumatoid human synovial tissues through utilization of Src-associated substrate during mitosis of 68 kDa (Sam68) thus enhances NF- κ B and IL-6 signaling. In turn, NF- κ B upregulates the TNF- α expression proposing an interdependence of sustained NF- κ B activation and TNF- α production. Interestingly, the anti-TNF- α effect of DSM and NMS in the present study may be direct thwart to TNF- α production by α -methylene- γ -lactone moiety (Chooodej et al., 2018) or secondary to the direct binding to NF- κ B. As previously pointed, TNF- α regulates IL-6 and MCP-1 production via NF- κ B that is not implemented efficiently without the presence of active GSK3 β (Steinbrecher et al., 2005). The present study showed the ability of NMS and DSM to block GSK3 β activation. This set the potential anti-arthritic character of DSM and NMS. This is in concordance with the previous studies that depicted the administration of GSK3 β inhibitor is accompanied with amelioration of arthritis features in rat model (Zhou et al., 2016). Although GSK3 β activity is inversely related to Akt activation but the present results demonstrated the ability of DSM and NMS in inhibition of GSK3 β in Akt-independent manner. One of pseudoguaianolide SLs structurally similar to DSM and NMS; helenalin activated protein kinase C, one of upstream inhibitors of GSK3 β , in cancer cell line (Kim et al., 2005). This may rationalize DSM-and NMS- induced inhibition of GSK3 β .

The overexpressed Cyr61 in RA patients coordinates cell proliferation and inflammatory cytokines production. Through its integrin receptor, Cyr61 proliferates cell with Akt activation and this puts Cyr61/Akt pathway as a culprit in the pathogenesis of RA pannus and joint destruction (Men et al., 2003; Zhang et al., 2009). Concerning cytokines production, Cyr61 mediates IL-6 production which implicated in the inflammatory milieu thereafter. Concomitantly, TNF- α stimulates Akt to inhibit negative regulation of transcription factor FOXO3a on Cyr61 expression from synovial fibroblasts of RA patients (Kok et al., 2013). Herein, for the first time, the present results demonstrate the anti-inflammatory and immunomodulatory effects of DSM and NMS due to curbing Cyr61 level. Our results comply with Zhai et al. (2017) who depicted the beneficial effect of anti-Cyr61 monoclonal antibodies in arthritis mouse model. On the basis of this study, the ability of SL to hamper the Cyr61 production may be partially via suppression of Akt-mediated inhibition of FOXO3a or its upstream; TNF- α .

IL-6 is the main pleiotropic cytokine, it is involved in immune response and cartilage destruction at the early phase of RA. Concomitantly, its serum level was fairly elevated and correlated to synovitis and cartilage damage (Saleem et al., 2020). Alongside, it is stated that Akt/NF- κ B signaling pathway mediates Cyr61-evoked IL-6 production in isolated FLS from RA patients (Lin et al., 2012). Moreover, NF- κ B is the intriguing factor for IL-6 production as demonstrated in fibroblasts with deleted NF- κ B p50/p65 genes that failed to express IL-6 (Georganas et al., 2000). One of the notable finding in this study is the DSM- and NMS-induced suppression of IL-6 level. This may be accounted to inhibition of NF- κ B, Akt and Cyr61. Xu et al. (2007) justified the anti-arthritic property of artesunate, one of SL derivatives, to its predominance on Akt and NF- κ B signaling pathway that subsequently inhibits TNF- α induced IL-6 production in human FLS.

Intracellularly, IL-6 activates 2 signaling pathways; SHP2/ERK1/2 and JAK/STAT-3 (Hirano et al., 2000). The first signaling, IL-6 utilizes STAT3 to implement inflammation in joints (Jones et al., 2013), whereas such biological action is confirmed by the presence of active p-STAT3 in synovia of RA patients (Wang et al., 1995) and reversed by IL-6 blocker (Ortiz et al., 2015). One of the promising results in this study is the mitigation of phosphorylated form of STAT3 by DSM and NMS. Similarly, researchers confirmed the inverse link between SLs and STAT3

phosphorylation at Tyr705 in cell lines that ceased IL-6-induced inflammation through blocking STAT3 activation and nuclear translocation (Sobota et al., 2000). On the other hand, phosphorylation of STAT3 is under control of active GSK3 β (Beurel and Jope, 2009). In this regard, it is likely in this study that the diminished paw p-STAT3 might be attributable to direct effect of SL or indirect via inhibition of Akt, GSK3 β and IL-6 level. Likewise, Basu et al. (2017) found IL-6/NF- κ B as another inflammatory signaling cascade for IL-6 in carrageenan paw model. This interdependence creates persistent NF- κ B activation. Inevitably, SL-induced deactivation of the two downstream transcription factors viz; NF- κ B and STAT3 may rationalize the promising anti-inflammatory effect of DSM and NMS. The anti-proliferative effect of DSM was witnessed in cancer cell lines via inhibition of STAT3 and NF- κ B (Villagomez et al., 2013).

The second IL-6 signaling; ERK1/2 appears as a candidate druggable target that is crucial for innate and adaptive immunity activation in arthritis. Using *in vitro* and *in vivo* models (Zhu et al., 2013) showed the mediatory role of ERK1/2 during the Cyr61-induced neutrophil infiltration into the inflamed joints. As well, it is involved in MCP-1 production thus attracts monocytes in RA (Chen et al., 2017). Herein, DSM and NMS purveyed their immunomodulatory ability through dephosphorylation of paw ERK1/2. In line with this finding, Ji et al. (2016) attributed the anti-inflammatory effect of SL in mouse macrophage to its role in inhibiting ERK1/2 signaling pathway which consequently blocked IL-6 and TNF- α signaling pathways. This found the immunomodulatory of DSM and NMS that may be in partial due to decline in IL-6, Cyr61 or TNF- α levels. Collectively, Monocyte chemoattractant namely; MCP-1 and TNF beside Akt and ERK1/2 are involved in monocyte trafficking in synovial fluid that destroy cartilage and bone in RA (Chen et al., 2013). This may elucidate the protective effect of DSM and NMS against damaged cartilage as observed in histopathological examination of the present study that may be partially due to ERK1/2, Akt and MCP-1 inhibition.

The masterpieces of arthritis milieu; NF- κ B and Cyr61/ERK1/2 signaling are integrated in MCP-1 production in RA (Chen et al., 2017; Makarov, 2001). which subsequently magnetizes monocytes in synovial fluid, serum and stromal cells of arthritis patients (Hayashida et al., 2001; Koch et al., 1992). These evidences feature the inflammatory and immunological roles of MCP-1. The present study afforded the anti-inflammatory and immunomodulatory effects of DSM and NMS through downregulating MCP-1 gene expression in CFA model. In harmony, it has been verified in *in vitro* and *in vivo* studies that inhibition of MCP-1 expression was one of the core anti-inflammatory mechanisms of SL even in low concentrations and a dose-dependent manner (Gao et al., 2017; Grassl et al., 2005; Qin et al., 2016). Concomitantly Svensson et al. (2018b), evinced DSM-evoked downregulation of IL-6 and MCP-1 expressions in human skin cells was via NF- κ B inhibition. Thus, the inhibitory action of DSM and NMS on Akt/NF- κ B, may be at least partially accounting for the decreased MCP-1.

Finally, to the best of our knowledge the findings of the current study provide the first report for the anti-arthritic effect of DSM and NMS that was designed by its immunomodulatory, anti-proliferating and anti-inflammatory characters that protect joint against autoimmune destruction instigated by CFA. Thus, this is offering a new perspective for the potential role of pseudoguaianolide SLs in RA.

References

- Abdelgaleil, S., Badawy, M., Sukanuma, T., Kitahara, K., 2011. Antifungal and biochemical effects of pseudoguaianolide sesquiterpenes isolated from *Ambrosia maritima* L. Afr. J. Microbiol. Res. 5 (21), 3385–3393.
- Abdelgaleil, S.A.M., Badawy, M.E.L., T. S., K. K., 2011. Antifungal and biochemical effects of pseudoguaianolide sesquiterpenes isolated from *Ambrosia maritima* L. Afr. J. Microbiol. Res. 5, 3385–3392.
- Ahmed, M.B., Khater, M.R., 2001. Evaluation of the protective potential of *Ambrosia maritima* extract on acetaminophen-induced liver damage. J. Ethnopharmacol. 75 (2–3), 169–174.

- Aletaha, D., Smolen, J.S., 2018. Diagnosis and management of rheumatoid arthritis: a review. *Jama* 320 (13), 1360–1372.
- Bartok, B., Boyle, D.L., Liu, Y., Ren, P., Ball, S.T., Bugbee, W.D., Rommel, C., Firestein, G.S., 2012. PI3 kinase δ is a key regulator of synovioyte function in rheumatoid arthritis. *Am. J. Pathol.* 180 (5), 1906–1916.
- Basu, A., Das, A.S., Sharma, M., Pathak, M.P., Chattopadhyay, P., Biswas, K., Mukhopadhyay, R., 2017. STAT3 and NF- κ B are common targets for kaempferol-mediated attenuation of COX-2 expression in IL-6-induced macrophages and carrageenan-induced mouse paw edema. *Biochem. Biophys. Res. Commun.* 491, 54–61.
- Berdan, C.A., Ho, R., Lehtola, H.S., To, M., Hu, X., Huffman, T.R., Petri, Y., Altobelli, C.R., Demeulenaere, S.G., Olzmann, J.A., Maimone, T.J., Nomura, D.K., 2019. Parthenolide covalently targets and inhibits focal adhesion kinase in breast cancer cells. *Cell Chem. Biol.* 26 (7), 1027–1035 e1022.
- Beurel, E., Jope, R.S., 2009. Lipopolysaccharide-induced interleukin-6 production is controlled by glycogen synthase kinase-3 and STAT3 in the brain. *J. Neuroinflammation* 6 (1), 9.
- Calabresi, E., Petrelli, F., Bonifacio, A., Puxeddu, I., Alunno, A., 2018. One year in review 2018: pathogenesis of rheumatoid arthritis. *Clin. Exp. Rheumatol.* 36 (2), 175–184.
- Chen, C.-Y., Fuh, L.-J., Huang, C.-C., Hsu, C.-J., Su, C.-M., Liu, S.-C., Lin, Y.-M., Tang, C.-H., 2017. Enhancement of CCL2 expression and monocyte migration by CCN1 in osteoblasts through inhibiting miR-518a-5p: implication of rheumatoid arthritis therapy. *Sci. Rep.* 7 (1), 421.
- Chen, Z., Kim, S.-j., Chamberlain, N.D., Pickens, S.R., Volin, M.V., Volkov, S., Arami, S., Christman, J.W., Prabhakar, B.S., Swedler, W., 2013. The novel role of IL-7 ligation to IL-7 receptor in myeloid cells of rheumatoid arthritis and collagen-induced arthritis. *J. Immunol.* 190 (10), 5256–5266.
- Chin, Y.R., Tokar, A., 2009. Function of Akt/PKB signaling to cell motility, invasion and the tumor stroma in cancer. *Cell. Signal.* 21 (4), 470–476.
- Choodej, S., Pudhom, K., Mitsunaga, T., 2018. Inhibition of TNF- α -induced inflammation by sesquiterpene lactones from *Saussurea lappa* and semi-synthetic analogues. *Planta Med.* 84, 329–335, 05.
- Deuis, J.R., Dvorakova, L.S., Vetter, I., 2017. Methods used to evaluate pain behaviors in rodents. *Front. Mol. Neurosci.* 10, 284.
- Doskotch, R.W., Hufford, C.D., 1969. Damsin, the cytotoxic principle of *Ambrosia ambrosioides* (cav.) payne. *J. Pharmaceut. Sci.* 58 (2), 186–188.
- Drury, R., Wallington, E., 1983. *1967Carleton's Histological Technique*. Oxford University Press, New York.
- Gao, S., Wang, Q., Tian, X.-H., Li, H.-L., Shen, Y.-H., Xu, X.-K., Wu, G.-Z., Hu, Z.-L., Zhang, W.-D., 2017. Total sesquiterpene lactones prepared from *Inula helenium* L. has potentials in prevention and therapy of rheumatoid arthritis. *J. Ethnopharmacol.* 196, 39–46.
- García-Piñeres, A.J., Castro, V.c, Mora, G., Schmidt, T.J., Strunck, E., Pahl, H.L., Merfort, I., 2001. Cysteine 38 in p65/NF- κ B plays a crucial role in DNA binding inhibition by sesquiterpene lactones. *J. Biol. Chem.* 276 (43), 39713–39720.
- García-Piñeres, A.J., Lindenmeyer, M.T., Merfort, I., 2004. Role of cysteine residues of p65/NF- κ B on the inhibition by the sesquiterpene lactone parthenolide and N-ethyl maleimide, and on its transactivating potential. *Life Sci.* 75 (7), 841–856.
- García, S., Liz, M., Gómez-Reino, J.J., Conde, C., 2010. Akt activity protects rheumatoid synovial fibroblasts from Fas-induced apoptosis by inhibition of Bid cleavage. *Arthritis Res. Ther.* 12 (1), R33.
- Georganas, C., Liu, H., Perlman, H., Hoffmann, A., Thimmapaya, B., Pope, R.M., 2000. Regulation of IL-6 and IL-8 expression in rheumatoid arthritis synovial fibroblasts: the dominant role for NF- κ B but not C/EBP β or c-Jun. *J. Immunol.* 165 (12), 7199–7206.
- Gong, J.-H., Ratkay, L.G., Waterfield, J.D., Clark-Lewis, I., 1997. An antagonist of monocyte chemoattractant protein 1 (MCP-1) inhibits arthritis in the MRL-lpr mouse model. *J. Exp. Med.* 186 (1), 131–137.
- Granado, M., Priego, T., Martín, A.I., Villanúa, M.Á., López-Calderón, A., 2005. Ghrelin receptor agonist GHRP-2 prevents arthritis-induced increase in E3 ubiquitin-ligating enzymes MuRF1 and MAFbx gene expression in skeletal muscle. *Am. J. Physiol. Endocrinol. Metabol.* 289 (6), E1007–E1014.
- Grassl, G.A., Fessele, S., Merfort, I., Lindenmeyer, M.T., Castro, V., Murillo, R., Nelson, P.J., Autenrieth, I.B., 2005. Sesquiterpene lactones inhibit *Yersinia* invasively protein-induced IL-8 and MCP-1 production in epithelial cells. *Int. J. Med. Microbiol.* 295 (8), 531–538.
- Guo, Q., Wang, Y., Xu, D., Nossent, J., Pavlos, N.J., Xu, J., 2018. Rheumatoid arthritis: pathological mechanisms and modern pharmacologic therapies. *Bone Res.* 6 (1), 1–14.
- Haas, C.S., Creighton, C.J., Pi, X., Maine, I., Koch, A.E., Haines III, G.K., Ling, S., Chinnaiyan, A.M., Holoshitz, J., 2006. Identification of genes modulated in rheumatoid arthritis using complementary DNA microarray analysis of lymphoblastoid B cell lines from disease-discordant monozygotic twins. *Arthritis Rheum.: Off. J. Am. College Rheumatol.* 54 (7), 2047–2060.
- Hayashida, K., Nanki, T., Girschick, H., Yavuz, S., Ochi, T., Lipsky, P.E., 2001. Synovial stromal cells from rheumatoid arthritis patients attract monocytes by producing MCP-1 and IL-8. *Arthritis Res. Ther.* 3 (2), 118.
- Hehner, S.P., Heinrich, M., Bork, P.M., Vogt, M., Ratter, F., Lehmann, V., Schulze-Osthoff, K., Dröge, W., Schmitz, M.L., 1998. Sesquiterpene lactones specifically inhibit activation of NF- κ B by preventing the degradation of I κ B- α and I κ B- β . *J. Biol. Chem.* 273 (3), 1288–1297.
- Hirano, T., Ishihara, K., Hibi, M., 2000. Roles of STAT3 in mediating the cell growth, differentiation and survival signals relayed through the IL-6 family of cytokine receptors. *Oncogene* 19 (21), 2548.
- Ivanescu, B., Miron, A., Corciova, A., 2015. Sesquiterpene lactones from *Artemisia* genus: biological activities and methods of analysis. *J. Anal. Methods Chem.* 2015.
- Ji, G.-Q., Chen, R.-Q., Wang, L., 2016. Anti-inflammatory activity of atractylenolide III through inhibition of nuclear factor- κ B and mitogen-activated protein kinase pathways in mouse macrophages. *Immunopharmacol. Immunotoxicol.* 38 (2), 98–102.
- Jones, G.W., Greenhill, C.J., Williams, J.O., Nowell, M.A., Williams, A.S., Jenkins, B.J., Jones, S.A., 2013. Exacerbated inflammatory arthritis in response to hyperactive gp130 signalling is independent of IL-17A. *Ann. Rheum. Dis.* 72 (10), 1738–1742.
- Kane, L.P., Shapiro, V.S., Stokoe, D., Weiss, A., 1999. Induction of NF- κ B by the Akt/PKB kinase. *Curr. Biol.* 9 (11), 601–601.
- Khansai, M., Phitak, T., Klangjorhor, J., Udornrak, S., Fanhchaksai, K., Pothacharoen, P., Kongtawelert, P., 2017. Effects of sesamin on primary human synovial fibroblasts and SW982 cell line induced by tumor necrosis factor- α as a synovitis-like model. *BMC Compl. Alternative Med.* 17 (1), 532.
- Kim, S.H., Oh, S.M., Kim, T.S., 2005. Induction of human leukemia HL-60 cell differentiation via a PKC/ERK pathway by helenalin, a pseudoguanolide sesquiterpene lactone. *Eur. J. Pharmacol.* 511 (2–3), 89–97.
- Koch, A.E., Kunkel, S.L., Harlow, L.A., Johnson, B., Evanoff, H.L., Haines, G.K., Burdick, M.D., Pope, R.M., Strieter, R.M., 1992. Enhanced production of monocyte chemoattractant protein-1 in rheumatoid arthritis. *J. Clin. Invest.* 90 (3), 772–779.
- Kok, S.H., Lin, L.D., Hou, K.L., Hong, C.Y., Chang, C.C., Hsiao, M., Wang, J.H., Lai, E.H. H., Lin, S.K., 2013. Simvastatin inhibits cysteine-rich protein 61 expression in rheumatoid arthritis synovial fibroblasts through the regulation of sirtuin-1/FoxO3a signaling. *Arthritis Rheum.* 65 (3), 639–649.
- Li, H., Guan, S.B., Lu, Y., Wang, F., Liu, Y.H., Liu, Q.Y., 2018. Genetic deletion of GIT2 prolongs functional recovery and suppresses chondrocyte differentiation in rats with rheumatoid arthritis. *J. Cell. Biochem.* 119 (2), 1538–1547.
- Lin, J., Zhou, Z., Huo, R., Xiao, L., Ouyang, G., Wang, L., Sun, Y., Shen, B., Li, D., Li, N., 2012. Cyr61 induces IL-6 production by fibroblast-like synoviocytes promoting Th17 differentiation in rheumatoid arthritis. *J. Immunol.* 188 (11), 5776–5784.
- Livak, K.J., Schmittgen, T.D., 2001. Analysis of relative gene expression data using real-time quantitative PCR and the 2⁻ $\Delta\Delta$ CT method. *Methods* 25 (4), 402–408.
- Lyß, G., Knorre, A., Schmidt, T.J., Pahl, H.L., Merfort, I., 1998. The anti-inflammatory sesquiterpene lactone helenalin inhibits the transcription factor NF- κ B by directly targeting p65. *J. Biol. Chem.* 273 (50), 33508–33516.
- Makarov, S.S., 2001. NF- κ B in rheumatoid arthritis: a pivotal regulator of inflammation, hyperplasia, and tissue destruction. *Arthritis Res. Ther.* 3 (4), 200.
- Malemud, C.J., 2015. The PI3K/Akt/Pten/mTOR pathway: a fruitful target for inducing cell death in rheumatoid arthritis? *Future Med. Chem.* 7 (9), 1137–1147.
- Martin, M., Rehani, K., Jope, R.S., Michalek, S.M., 2005. Toll-like receptor-mediated cytokine production is differentially regulated by glycogen synthase kinase 3. *Nat. Immunol.* 6 (8), 777.
- Men, J., Mehmi, I., Griggs, D., Lupu, R., 2003. The angiogenic factor CYR61 in breast cancer: molecular pathology and therapeutic perspectives. *Endocr. Relat. Canc.* 10 (2), 141–152.
- Ortiz, M., Díaz-Torné, C., Hernández, M., Reina, D., de la Fuente, D., Castellvi, I., Moya, P., Ruiz, J., Corominas, H., Zamora, C., 2015. IL-6 blockade reverses the abnormal STAT activation of peripheral blood leukocytes from rheumatoid arthritis patients. *Clin. Immunol.* 158 (2), 174–182.
- Pap, T., Franz, J.K., Hummel, K.M., Jeisy, E., Gay, R., Gay, S., 1999. Activation of synovial fibroblasts in rheumatoid arthritis: lack of expression of the tumour suppressor PTEN at sites of invasive growth and destruction. *Arthritis Res. Ther.* 2 (1), 59.
- Pearson, C.M., 1964. Experimental models in rheumatoid disease. *Arthritis Rheum.: Off. J. Am. College Rheumatol.* 7 (1), 80–86.
- Qin, X., Jiang, X., Jiang, X., Wang, Y., Miao, Z., He, W., Yang, G., Lv, Z., Yu, Y., Zheng, Y., 2016. Micheliolide inhibits LPS-induced inflammatory response and protects mice from LPS challenge. *Sci. Rep.* 6, 23240.
- Rantapää-Dahlqvist, S., Boman, K., Tarkowski, A., Hallmans, G., 2007. Up regulation of monocyte chemoattractant protein-1 expression in anti-citrulline antibody and immunoglobulin M rheumatoid factor positive subjects precedes onset of inflammatory response and development of overt rheumatoid arthritis. *Ann. Rheum. Dis.* 66 (1), 121–123.
- Rubbert-Roth, A., Finckh, A., 2009. Treatment options in patients with rheumatoid arthritis failing initial TNF inhibitor therapy: a critical review. *Arthritis Res. Ther.* 11 (1), S1.
- Saad, M.A., El-Sahhar, A.E., Arab, H.H., Al-Shorbagy, M.Y., 2019. Nicorandil abates arthritic perturbations induced by complete Freund's adjuvant in rats via conquering TLR4-MyD88-TRAF6 signaling pathway. *Life Sci.* 218, 284–291.
- Saeed, M., Jacob, S., Sandjo, L.P., Sugimoto, Y., Khalid, H.E., Opatz, T., Thines, E., Effert, T., 2015. Cytotoxicity of the sesquiterpene lactones neoambrosin and damsin from *Ambrosia maritima* against multidrug-resistant cancer cells. *Front. Pharmacol.* 6, 267.
- Saleem, A., Saleem, M., Akhtar, M.F., Shahzad, M., Jahan, S., 2020 Mar. *Polystichum braunii* extracts inhibit Complete Freund's adjuvant-induced arthritis via upregulation of I- κ B, IL-4, and IL-10, downregulation of COX-2, PGE2, IL-1 β , IL-6, NF- κ B, and TNF- α , and subsiding oxidative stress. *Inflammopharmacology*. <https://doi.org/10.1007/s10787-020-00688-5>.
- Schepetkin, I.A., Kirpotina, L.N., Mitchell, P.T., Kishkentaeva, A.S., Shaimerdenova, Z.R., Atazhanova, G.A., Adekenov, S.M., Quinn, M.T., 2018. The natural sesquiterpene lactones arglabin, grosheimin, agracin, parthenolide, and estafiatin inhibit T cell receptor (TCR) activation. *Phytochemistry* 146, 36–46.
- Simmonds, R.E., Foxwell, B.M., 2008. Signalling, inflammation and arthritis: NF- κ B and its relevance to arthritis and inflammation. *Rheumatology* 47 (5), 584–590.
- Sobota, R., Szwed, M., Kasza, A., Bugno, M., Kordula, T., 2000. Parthenolide inhibits activation of signal transducers and activators of transcription (STATs) induced by cytokines of the IL-6 family. *Biochem. Biophys. Res. Commun.* 267 (1), 329–333.

- Stein, C., Millan, M., Herz, A., 1988. Unilateral inflammation of the hindpaw in rats as a model of prolonged noxious stimulation: alterations in behavior and nociceptive thresholds. *Pharmacol. Biochem. Behav.* 31 (2), 445–451.
- Steinbrecher, K.A., Wilson, W., Cogswell, P.C., Baldwin, A.S., 2005. Glycogen synthase kinase 3 β functions to specify gene-specific, NF- κ B-dependent transcription. *Mol. Cell Biol.* 25 (19), 8444–8455.
- Sun, W., Qin, R., Wang, R., Ding, D., Yu, Z., Liu, Y., Hong, R., Cheng, Z., Wang, Y., 2018. Sam68 promotes invasion, migration, and proliferation of fibroblast-like synoviocytes by enhancing the NF- κ B/P65 pathway in rheumatoid arthritis. *Inflammation* 41 (5), 1661–1670.
- Svensson, D., Lozano, M., Almanza, G.R., Nilsson, B.-O., Sterner, O., Villagomez, R., 2018a. Sesquiterpene lactones from *Ambrosia arborescens* Mill. inhibit pro-inflammatory cytokine expression and modulate NF- κ B signaling in human skin cells. *Phytomedicine*.
- Svensson, D., Lozano, M., Almanza, G.R., Nilsson, B.-O., Sterner, O., Villagomez, R., 2018b. Sesquiterpene lactones from *Ambrosia arborescens* Mill. inhibit pro-inflammatory cytokine expression and modulate NF- κ B signaling in human skin cells. *Phytomedicine* 50, 118–126.
- Thalhamer, T., McGrath, M., Harnett, M., 2008. MAPKs and their relevance to arthritis and inflammation. *Rheumatology* 47 (4), 409–414.
- Villagomez, R., Collado, J., Muñoz, E., Almanza, G., Sterner, O., 2014. Natural and semi-synthetic pseudoguaianolides as inhibitors of NF- κ B. *J. Biomed. Sci. Eng.* (7), 833–847.
- Villagomez, R., Hatti-Kaul, R., Sterner, O., Almanza, G., Linares-Pastén, J.A., 2015. Effect of natural and semisynthetic pseudoguaianolides on the stability of NF- κ B: DNA complex studied by agarose gel electrophoresis. *PLoS One* 10 (1), e0115819.
- Villagomez, R., Rodrigo, G.C., Collado, I.G., Calzado, M.A., Muñoz, E., Åkesson, B., Sterner, O., Almanza, G.R., Duan, R.-D., 2013. Multiple anticancer effects of damsin and coronopilin isolated from *Ambrosia arborescens* on cell cultures. *Anticancer Res.* 33 (9), 3799–3805.
- Wang, F., Sengupta, T.K., Zhong, Z., Ivashkiv, L.B., 1995. Regulation of the balance of cytokine production and the signal transducer and activator of transcription (STAT) transcription factor activity by cytokines and inflammatory synovial fluids. *J. Exp. Med.* 182 (6), 1825–1831.
- Xu, H., He, Y., Yang, X., Liang, L., Zhan, Z., Ye, Y., Yang, X., Lian, F., Sun, L., 2007. Antimalarial Agent Artesunate Inhibits TNF- α -Induced Production of Proinflammatory Cytokines via Inhibition of NF- κ B and PI3 kinase/Akt Signal Pathway in Human Rheumatoid Arthritis Fibroblast-like Synoviocytes.
- Yoshida, Y., Tanaka, T., 2014. Interleukin 6 and rheumatoid arthritis. *BioMed Res. Int.* 2014.
- Youl Cho, J., 2006. Sesquiterpene lactones as a potent class of NF- κ B activation inhibitors. *Curr. Enzym. Inhib.* 2 (4), 329–341.
- Zhai, T., Gao, C., Huo, R., Sheng, H., Sun, S., Xie, J., He, Y., Gao, H., Li, H., Zhang, J., 2017. Cyr61 participates in the pathogenesis of rheumatoid arthritis via promoting MMP-3 expression by fibroblast-like synoviocytes. *Mod. Rheumatol.* 27 (3), 466–475.
- Zhang, H.G., Wang, Y., Xie, J.F., Liang, X., Liu, D., Yang, P., Hsu, H.C., Ray, R., Mountz, J.D., 2001. Regulation of tumor necrosis factor α -mediated apoptosis of rheumatoid arthritis synovial fibroblasts by the protein kinase Akt. *Arthritis Rheum.: Off. J. Am. College Rheumatol.* 44 (7), 1555–1567.
- Zhang, Q., Wu, J., Cao, Q., Xiao, L., Wang, L., He, D., Ouyang, G., Lin, J., Shen, B., Shi, Y., 2009. A critical role of Cyr61 in interleukin-17-dependent proliferation of fibroblast-like synoviocytes in rheumatoid arthritis. *Arthritis & Rheumatism: Off. J. Am. College Rheumatol.* 60 (12), 3602–3612.
- Zhou, H., Liu, J., Zeng, J., Hu, B., Fang, X., Li, L., 2016. Inhibition of GSK-3 β alleviates collagen II-induced rheumatoid arthritis in rats. *Med. Sci. Mon. Int. Med. J. Exp. Clin. Res.: int. Med. J. Exp. Clin. Res.* 22, 1047.
- Zhu, X., Xiao, L., Huo, R., Zhang, J., Lin, J., Xie, J., Sun, S., He, Y., Sun, Y., Zhou, Z., 2013. Cyr61 is involved in neutrophil infiltration in joints by inducing IL-8 production by fibroblast-like synoviocytes in rheumatoid arthritis. *Arthritis Res. Ther.* 15 (6), R187.